The Aperture Problem for Refractive Motion

Tianfan Xue, Hossein Mobahi, Frédo Durand, and William T. Freeman
MIT Computer Science and Artificial Intelligence Laboratory
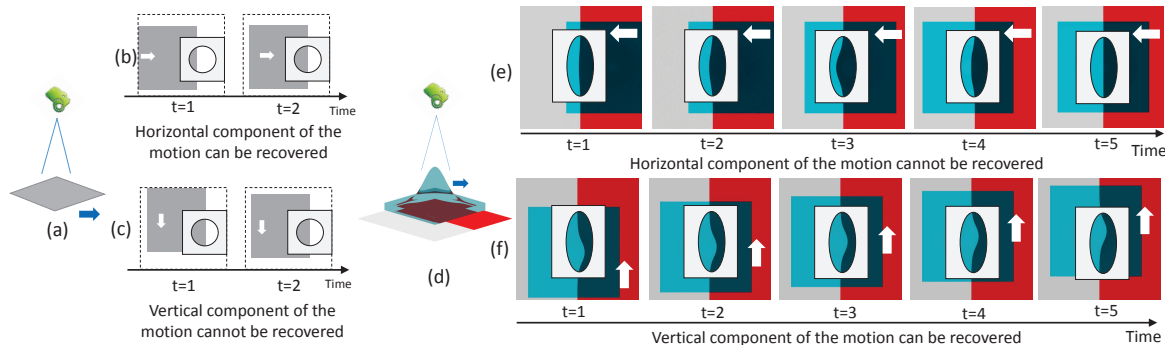{tfxue,hmobahi,fredo,billf}@mit.edu

Figure 1. **The aperture problem for an opaque object**. (a) A camera is imaging an opaque moving object (gray). (b) When a vertical edge is observed within the aperture (the white circular mask), we can resolve the horizontal component of the motion. (c) The vertical component of the motion is ambiguous, because when the object moves vertically, no change is observed through this aperture. **The aperture problem for a refractive object**. (d) A camera is viewing a stationary and planar background (white and red) through a moving Gaussian-shaped glass (blue). (e) The horizontal motion is ambiguous, because the observed sequence is symmetric. That is, if the glass moves in the opposite direction, the same sequence will be observed. (f) The vertical motion can be recovered, e.g. by tracking the observed tip of the bump.

Abstract

When viewed through a small aperture, a moving image provides incomplete information about the local motion. Only the component of motion along the local image gradient is constrained. In an essential part of optical flow algorithms, information must be aggregated from nearby image locations in order to estimate all components of motion. This limitation of local evidence for estimating optical flow is called "the aperture problem".

We pose and solve a generalization of the aperture problem for moving refractive elements. We consider a common setup in air flow imaging or telescope observation: a camera is viewing a static background, and an unknown refractive elements undergoing unknown motion between them. Then we are addressing this fundamental question: what does the local image motion tell us about the motion of refractive elements?

We show that the information gleaned through a local aperture for this case is very different than that for optical flow. In optical flow, the movement of 1D structure already constrains the motion in a certain direction. However, we cannot infer any information about the refractive motion from the movement of 1D structure in the observed

sequence, and can only recover one component of the motion from 2D structure. Results on both simulated and real sequences are shown to illustrate our theory.

1. Introduction

Our visual system integrates many pieces of ambiguous local information to achieve a global scene interpretation. An example of a global percept inferred from such local data is motion. We unambiguously see objects moving coherently in the world, although the local motion signals may be ambiguous. The local ambiguous motion signals are studied under the name of the "aperture problem".

The traditional form of the aperture problem focuses on the motion of opaque objects. It describes the ambiguity of the inferred motions when the observing local image structures which only vary along one direction [3, 10, 4]. When the region of analysis–the aperture–becomes large enough, the image is likely to have a two-dimensional structure, and the motion ambiguity then disappears. Conversely, when the aperture is too small, the ambiguity is often present. This is illustrated in Figure 1(a,b,c) for a vertical edge surface. The local observation only

specifies the component of motion perpendicular to the edge boundary. Hence, any information related to the component of motion parallel to the edge is lost, which results in the ambiguity.

However, in our world, it is not only opaque objects that may move, but also refractive objects, such as glass or hot air. The traditional aperture theory cannot be applied to these objects, as they do not have their own images. But it is still possible to perceive the motion of these objects when they move against a textured background. This is because when an inhomogeneous or uneven refractive object moves in front of a background, the observed background will be distorted. Observing this distortion can reveal the motion of the refractive object.

While many motion estimation algorithms for refractive objects have been proposed [6, 15, 17, 19, 22, 30, 31] (see Section 1.1), a fundamental question remains unanswered: *what information about the world can we infer from local distortions caused by refractive motion*?

This topic cannot be addressed by the traditional aperture problem. In fact, motion analysis of refractive objects based on the traditional aperture problem can be quite misleading. For example, consider a stationary vertical edge observed through a small aperture. Assume a Gaussian-shaped glass moves between this background and the aperture, as shown in Figure 1(d). When the glass moves perpendicular to the edge boundary, as in Figure 1(e), the observed boundary first bulges to the left (t = 1,2,3), and then returns to the original shape (t = 3,4,5). Due to the symmetry in this observed sequence, reversing the motion of the glass produces the same observation. Therefore, from the observed sequence, we cannot infer whether the glass is moving toward or away from the edge boundary. This is opposite to the traditional aperture theory, which states the component of the motion perpendicular to the edge direction can be recovered (Figure 1(b)). On the other hand, here we can recover the vertical motion of the glass, as in Figure 1(f), by tracking the observed tip of the bump. This is again contrary to the traditional aperture theory, which observes that the component of the motion parallel to the edge cannot be recovered (Figure 1(c)).

When there is ambiguity in refractive flow estimation, estimated motion by existing algorithms will be incorrect. For example, Figure 2 shows a sequence taken through the upward hot air flow generated by the stove below. The motion this hot air flow is estimated from two regions (red rectangles) of this sequence, using the algorithm in [31]. When the background structure is vertical (parallel to the direction of air flow), the algorithm can correctly recover the air motion, as shown on the left. However, when the background structure is horizontal (perpendicular to the direction of air flow), the algorithm fails to find the correct air motion, as shown on the right.
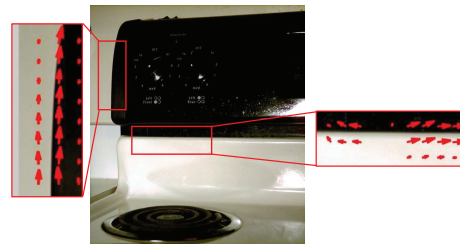

Figure 2. Revealing the aperture problem for refractive flow, see text.

In this paper, we will offer a theory for the aperture problem of refractive objects when it moves between a static camera and a static and opaque background. Following the tradition of the aperture problem, we choose the aperture small enough so that the background within that aperture is either uniform (purely black or white) or contains a single straight edge. Due to the non-uniform refraction, the observed shape through the aperture might be distorted. If the distortion is strong enough so that we observe a curved shape, we can recover the component of the motion parallel to the background structure, but we cannot recover the component perpendicular to it. Otherwise, we cannot infer anything about the motion. This is similar to the example shown in Figure 1. Results from both synthetic and real videos are presented to support the theoretical claim.

1.1. Related Work

Motion estimation of refractive objects is well studied. Two classic techniques used for refractive fluids are Particle Image Velocimetry (PIV) [5, 24] and Schlieren photography [16, 18, 25, 26, 27]. In PIV, the fluid motion is measured by tracking those tiny particles pre-inserted into the fluid. Schlieren photography is a technique to visualize the refractive fluid by exploring the change of the refraction index using a carefully tuned lens system. However, none of them are based on natural videos and our paper only focuses on motion estimation based on natural image sequences.

The technique whose setup is closest to that of our theory is "Background Oriented Schlieren" (BOS, a.k.a. Synthetic Schlieren) [14, 15, 17, 19, 21, 22, 30, 31, 9]. In this technique, a camera observes a textured background through a moving refractive fluid. The refractive fluid is visualized by estimating the changes between frames. While most of the works on BOS focus on visualizing the fluid flow, there are a few works that also estimate the fluid motion. Xue et al. [31] estimate the fluid motion by tracking the distortion of the observed sequence over time. Alterman [7] proposed to recover turbulence strength field using linear tomography. However, we are not aware of any theoretical analysis of local motion ambiguity for refractive objects, and our paper tries to fill this gap.

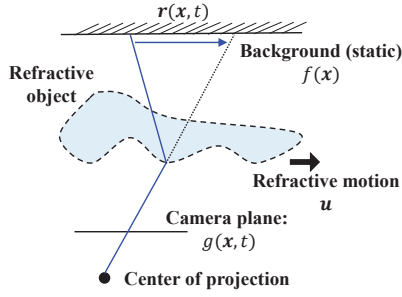In addition, there are a number of other works about

Figure 3. Image Formation Model

imaging under refraction that are worth to mention. The first line of work is reconstructing 3D shape of refractive objects from either a sequence or multi-view images. Several techniques are proposed to recover the surface of the water by imaging it in front of a textured background [32, 20, 13, 8]. Moreover, Agarwal et al. proposed an algorithm to recover both the motion of background and the shape of a refractive object, assuming the refractive object is static and background is moving [6]. Ben-Ezra and Nayar proposed a method to reconstruct the 3D geometry of a refractive object, assuming the refractive object and background are static and the camera is moving with known speed [11]. The main difference of these works to ours is that they are focusing on recovering the 3D geometry of the refractive objects, not its motion, and some of them even assume that refractive objects are static [6, 11].

The second set of papers study specular flow [1, 2, 12], to recover the shape of reflective object (instead of refractive object) from a sequence captured. Most of papers assume that the reflective object is static, and either the camera, background, or both, are moving. Because these works are about reflective objects, the image formation model is different than ours. In refraction, the angle between incident light and the outgoing light is small and high order terms can be ignored [31], thus it can be characterized as a 2D warping field, while in reflection, such an approximation fails and a more complicated formulation is needed.

Last but not least, there are several techniques to recover the undistorted background image from a distorted sequence taken through turbulent flow [23, 29, 33, 28], but we are not studying that problem.

2. Problem Definition

Image formation is modeled in the following way[1]. Consider any planar and static *background* pattern $f(\mathbf{x})$ and a camera observing it through a refractive layer, as shown in Figure 3. Denote *observed images* (over time) through the camera by $g(\mathbf{x}, t)$. For simplicity, let image coordinates be such that the observed image on the camera plane is the same as the background image when there is no refractive object, that is $g(\mathbf{x}, t) = f(\mathbf{x})$.

Now we add a refractive object between the camera and the background. This causes a distorted observation of the background through the camera. We model this distortion by an unknown warping field $\mathbf{r}(\mathbf{x}, t) = (r_x(\mathbf{x}, t), r_y(\mathbf{x}, t))$, which depends on the shape and index of refraction of the object. The distorted background captured by the camera obeys the following identity (see Figure 3),

$$g(\mathbf{x}, t) = f\big(\mathbf{x} - \mathbf{r}(\mathbf{x}, t)\big). \tag{1}$$

To gear the theory toward the physics of the real world, we leverage a few assumptions. Suppose the refractive object consists of small regions of uniform light bending power and each region moves with a constant speed $\mathbf{u}(\mathbf{x})$ in a short time around t_0, where $\mathbf{x}$ is the location of this piece at time t_0. Also suppose that the refraction caused by each small region is constant over some small time period. This assumption is referred to as refractive constancy assumption[2] in [31], and it approximates the behavior of both both rigid and fluid refractive objects. Based on this assumption, the warping field $\mathbf{r}$ can be expressed as:

$$\forall t \in \mathcal{N}(t_0); \; \mathbf{r}(\mathbf{x}, t) = \mathbf{r}_0(\mathbf{x} - \mathbf{u}(\mathbf{x})t), \tag{2}$$

where $\mathbf{r}_0$ is the refractive field at time t_0, i.e. $\mathbf{r}_0(\mathbf{x}) = \mathbf{r}(\mathbf{x}, t_0)$. By plugging Eq. 2 to Eq. 1, we obtain the **image formation equation**[3]:

$$\forall (\mathbf{x}, t) \in \mathcal{N}(\mathbf{x}_0, t_0); \; g(\mathbf{x}, t) = f(\mathbf{x} - \mathbf{r}_0(\mathbf{x} - \mathbf{u}t)). \tag{3}$$

The motion estimation task is to recover the motion $\mathbf{u}$ of the refractive object from the observed image sequence $g(\mathbf{x}, t)$, without knowing either the background image $f(\mathbf{x})$ or the refractive field $\mathbf{r}_0(\mathbf{x})$. Formally, given the observed image sequence $g(\mathbf{x}, t)$ within a small space-time window around $(\mathbf{x}_0, t_0)$, we want to find the solution space of the refractive motion:

$$\mathcal{U} = \{\mathbf{u} \,|\, \exists f, \mathbf{r}_0, \forall \mathbf{x}, t \,; \, g(\mathbf{x}, t) = f(\mathbf{x} - \mathbf{r}_0(\mathbf{x} - \mathbf{u}t))\}. \tag{4}$$

Ideally, $|\mathcal{U}|$ would contain a single element. Generally, however, the observed sequence may be explained by multiple motion vectors $|\mathcal{U}| > 1$, meaning the problem is ill-posed. Identifying such ambiguous cases and their associated solution space $\mathcal{U}$ is the goal of this paper. In the next section, we present a theory to improve our understanding about such ambiguities.

---

[1]Throughout the paper we denote a scalar as a, vector as $\mathbf{a}$, matrix as A, and a set as $\mathcal{A}$. We let $\mathcal{N}(\mathbf{a})$ be a small neighborhood of $\mathbf{a}$ and denote the 2D coordinate of a point on the image plane by the vector $\mathbf{x} = (x, y)$. All vectors, if not specified, are column vectors.

[2]This assumption on refractive objects is analogous to the brightness constancy of opaque objects, and it holds if the refractive angle is small.

[3]Since we assume $\mathbf{u}$ is constant within the aperture, we omit the spatial index $\mathbf{x}$ of $\mathbf{u}(\mathbf{x})$.
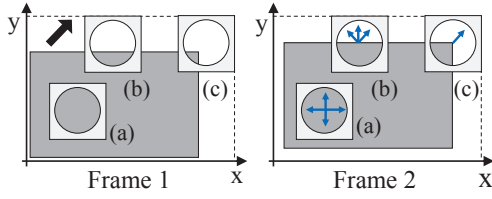
Figure 4. The aperture problem for opaque objects. A square object (marked by gray) is moving to the top-right, and we are trying to estimate the motion of this object from small apertures (a)-(c). A smooth region is observed through aperture (a), and we cannot get any information about the object motion, because any motion direction (marked by blue arrows) can explain the observation. A step edge is observed through (b), and we can infer that object is either moving to top-left, top, or top-right (marked by blue arrows). A "L shape" (2D structure) is observes through (c), and we can fully resolve the object motion.

Also, we assume that the background is only a step edge within the aperture (a spatiotemporal window around (x_0, t_0)), that is[4]:

$$f(\mathbf{x}) = \begin{cases} 0, & \text{if } \mathbf{n}^\mathsf{T}\mathbf{x} \leq 0 \\ 1, & \text{otherwise} \end{cases} \quad . \tag{5}$$

where $\mathbf{n}$ is the direction of background gradient. For simplicity, we use the following notation to denote the black-and-white background pattern described in Eq. 5:

$$f(\mathbf{x}) : \mathbf{n}^\mathsf{T}\mathbf{x} \leq 0. \tag{6}$$

Finally, we assume the refractive field is quadratic within the aperture:

$$\mathbf{r}_0(\mathbf{x}) = \bar{\mathbf{r}} + J\mathbf{x} + \frac{1}{2}\begin{pmatrix} \mathbf{x}^\mathsf{T} H_x \mathbf{x} \\ \mathbf{x}^\mathsf{T} H_y \mathbf{x} \end{pmatrix}. \tag{7}$$

where $\bar{\mathbf{r}} \in \mathbb{R}^2$ is the constant term, $J \in \mathbb{R}^{2 \times 2}$ is the Jacobian matrix of the refractive field $\mathbf{r}$, and $H_x, H_y \in \mathbb{R}^{2 \times 2}$ are Hessian matrices of x and y components of it.

3. Aperture Theory for Refractive Motion

The "aperture problem" describes the intrinsic ambiguity of perceiving the motion of an object through a local observation. Such ambiguity depends on the complexity of the structure observed through an aperture. This section presents a theory for characterizing the ambiguity space (Eq. 4) for the refractive motion.

The aperture problem for surface motion. In order to provide some context, we first review the traditional aperture problem for surface motion. The traditional aperture problem studies the motion of an *opaque* object

[4]The general equation of linear background should be $\mathbf{n}^\mathsf{T}\mathbf{x} + c \leq 0$. For simplicity, we ignore the bias term c. See the supplementary material for the full derivation.
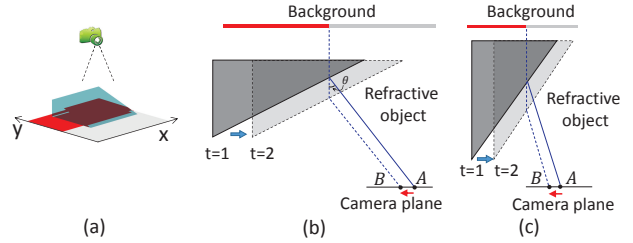

Figure 5. The ambiguity in motion estimation when only the first order structure is observed. A sequence is captured under the setup shown in (a), and cross sections along the y-direction under two different settings are shown in (b) and (c).

observed through a small aperture. The associated ambiguity of recovering motion is demonstrated in Figure 4. If the observed region is totally plain, as in Figure 4(a), then we cannot infer the motion of the object, and the solution space[5] of motion $\mathcal{U}$ is $\mathbb{R}^2$ velocity space. If only a straight edge (first order structure) is observed within the aperture, as shown in Figure 4(b), we can only resolve the component of the motion that is perpendicular to this edge, and the solution space $\mathcal{U}$ is a line in $\mathbb{R}^2$ velocity space. Finally, if a higher order structure is observed within the aperture (in Figure 4(c)), the ambiguity is fully resolved. This is summarized in the middle row of Table 1.

The refractive aperture problem. For refractive motion, we still discuss its ambiguity under three different classes of local observations: flat regions, first order structure (the boundary is a straight edge), and second order structure (the boundary is a conic curve).

When the background is totally plain, no matter how refractive object moves, we observe no change in the captured sequence. Therefore, *1. Observing a plain pattern (pure black or pure white) does not reveal any information about object's motion.*

The other two cases are more complicated, and in the following two sections we will show that: *2. the movement of a 1D structure in the observed sequence still does not reveal any information about object's motion, and 3. the movement of a 2D structure in the observed sequence reveals the motion in only one direction.*

3.1. First Order Observation

When a first order structure is observed, no information about refractive motion can be recovered. To illustrate this, consider the example shown in Figure 5. A camera is imaging a static edge-shaped background through a moving prism. The prism is oriented in the way that it has no variation along the x-direction. Therefore, the motion in

[5]With the abused of notation, here we also denote the solution space of the traditional aperture problem as $\mathcal{U}$.

Table 1. Comparison between the traditional aperture problem and the refractive aperture problem. $\mathcal{U}$ is the set of all possible solutions to object motion (either opaque objects or refractive objects) from the input sequence, and $\mathbf{u}^*$ is the ground truth motion.

The observed image sequence through the aperture	Constant	First order structure (a straight edge)	Second order structure (a conic curve)
The traditional aperture problem	$\mathcal{U} = \mathbb{R}^2$ (No information)	$\mathcal{U}$ is a line in $\mathbb{R}^2$	$\mathcal{U} = \{\mathbf{u}^*\}$
The refractive aperture problem	$\mathcal{U} = \mathbb{R}^2$ (No information)	$\mathcal{U} = \mathbb{R}^2$ (No information)	$\mathcal{U}$ is a line in $\mathbb{R}^2$

x-direction does not affect the observed sequence, which is similar to the traditional aperture problem.

In addition, the magnitude of the motion along the y-direction is also lost. To see that, consider a cross section along the y-direction (Figure. 5(b,c)). The projection of the background boundary moves from A to B due to the change of refraction.[6] The magnitude and the direction of this observed motion (red arrow in Figure 5) is related to both the motion of the refractive object and the angle of the prism. The same observed motion might be due to either a large motion of the prism and a small refraction (small angle) as in Figure 5(b), or to a small motion and a large refraction (large angle) as in Figure 5(c). Since both the motion and the shape of the refractive object are unknown, there is no way to resolve this ambiguity. Therefore, the ambiguity space $\mathcal{U}$ of refractive motion is the whole velocity space $\mathbb{R}^2$.

Mathematical derivation Now we will illustrate this ambiguity mathematically. Because only a first order structure is observed through the aperture, we can drop the second order term[7] in $\mathbf{r}$. Plugging the equation of background Eq. 5 and the equation of refractive field Eq. 7 into the image formation Eq. 3 (constant terms are omitted for simplicity):

$$g(\mathbf{x}, t) : \mathbf{x}^\mathsf{T}(I - J^\mathsf{T})\mathbf{n} - \mathbf{n}^\mathsf{T}\bar{\mathbf{r}} + \mathbf{n}^\mathsf{T}J\mathbf{u}t \qquad (8)$$

where I is the 2×2 identity matrix.

Eq. 8 is an equation of a line w.r.t. variable $\mathbf{x}$. Note that unknowns in Eq. 8 are $\mathbf{r}$, J, $\mathbf{n}$, and $\mathbf{u}$. It is easy to show that for any motion vector $\mathbf{u}$, we can design $\mathbf{r}$, J, and $\mathbf{n}$ such that

---

[6]Notice that the observed motion of image boundary on the image plane (marked by the red arrow) does not necessarily have the same direction as the motion of the refractive object (marked by the blue arrow).

[7]Second order term in $\mathbf{r}$ can be ignored because otherwise a curved pattern would have been observed instead of a straight edge.

they satisfy this line equation and hence generate the same observed sequence for the boundary (see supplementary material for detailed proof). Moreover, the speed of line is proportional to $\mathbf{n}^\mathsf{T}J\mathbf{u}$, which shows the same observed movement can either due to a large refraction (large J) and a small motion (small $\mathbf{u}$), or a small refraction (small $\mathbf{u}$) and a large motion (large $\mathbf{u}$). Therefore, we cannot recover any information about refractive motion $\mathbf{u}$ in this case.

3.2. Second Order Observation

For a refractive object, when we observe a second order through the aperture, we can only recover the motion in one direction. That means, the solution space $\mathcal{U}$ for the motion is reduced to a line in $\mathbb{R}^2$ velocity space.

To illustrate this, we revisit the Gaussian-shaped glass example discussed in the introduction.

First it is impossible to recover its the component of the motion perpendicular to the background structure. Figure 6(a) illustrates this ambiguity. Two different Gaussian glasses move towards opposite directions (the left column of Figure 6(a)). Due to the refraction, the background boundary moves away from its original location, and such distortion is illustrated by the red arrow in Figure 6(c). Also, one glass is a complementary of the other, so that they will bend the light passing towards opposite directions. Because the shapes of glasses are complementary and the motions of glasses are also opposite, the observed distortion within the aperture are actually similar (the right column of Figure 6(a)). Thus it is hard to infer the motion of the glass from observed distortion. The cause of this ambiguity is similar to the case of first order observation.

On the other hand, when the glass moves parallel to the background structure (Figure 6(b)), the observe boundary moves at the same speed as the glass. Now the movement of observed boundary does not depend on the shape of the
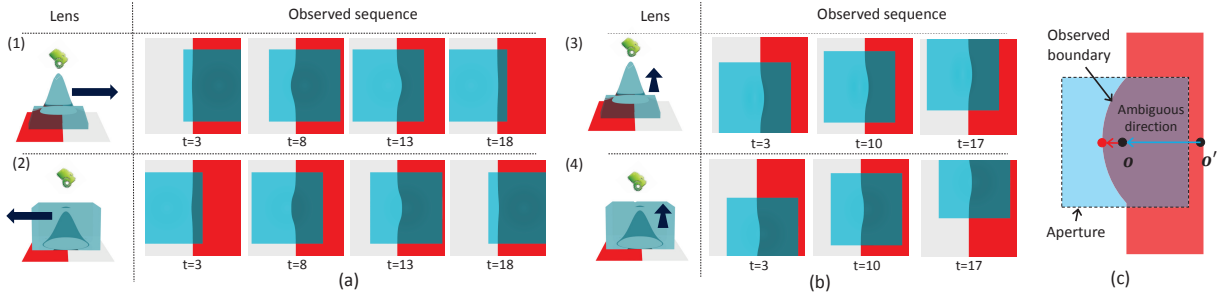
Figure 6. Ambiguity in motion estimation when a second order structure is observed, see text.

glass. Thus, we can infer the component of the glass motion that is parallel to the background structure by tracking the tip of the observed boundary (the red dot in Figure 6(c)).

Mathematical derivation Now we will explain the cause of such ambiguity. For simplicity, we assume that the Jacobian and Hessian of the refractive field are scalar matrices, which is true when the refractive object have a centroid-symmetric shape (like Gaussian-shape glasses shown in Figure 6). We will present the refractive flow equation for general case at the end of this section.

In the simplified case, the refractive field $\mathbf{r}$ can be represented as:

$$\mathbf{r}_0(\mathbf{x}) = \bar{\mathbf{r}} + j\mathbf{x} + \frac{1}{2}\left(\begin{array}{c} h_x\mathbf{x}^\mathsf{T}\mathbf{x} \\ h_y\mathbf{x}^\mathsf{T}\mathbf{x} \end{array}\right), \quad (9)$$

where $J = jI, H_x = h_xI, H_y = h_yI$[8]. Then the image formation Eq. 3 becomes (plugs Eq. 5 and Eq. 9 into Eq. 3):

$$g(\mathbf{x}, t) : -\frac{h}{2}\mathbf{x}^\mathsf{T}\mathbf{x} + (h\mathbf{u}t + \mathbf{n} - j\mathbf{n})^\mathsf{T}\mathbf{x} + j\mathbf{n}^\mathsf{T}\mathbf{u}t + d - \frac{h}{2}\mathbf{u}^\mathsf{T}\mathbf{u}t^2, \quad (10)$$

where $\mathbf{n} = [n_x, n_y]$, $h = h_xn_x + h_yn_y$, and $d = -\mathbf{n}^\mathsf{T}\bar{\mathbf{r}}$.

Eq. 10 is an equation of a circle $a(t)\mathbf{x}^\mathsf{T}\mathbf{x} + \mathbf{q}(t)^\mathsf{T}\mathbf{x} + 1 = 0$, and we can get its parameters $a(t)$ and $\mathbf{q}(t)$ by circle fitting:

$$\begin{cases} a(t) = -\frac{h}{2(j\mathbf{n}^\mathsf{T}\mathbf{u}t + d - \frac{h}{2}\mathbf{u}^\mathsf{T}\mathbf{u}t^2)}, \\ \mathbf{q}(t) = \frac{h\mathbf{u}t + \mathbf{n} - j\mathbf{n}}{j\mathbf{n}^\mathsf{T}\mathbf{u}t + d - \frac{h}{2}\mathbf{u}^\mathsf{T}\mathbf{u}t^2}. \end{cases} \quad (11)$$

Note that except $a(t)$ and $\mathbf{q}(t)$, all other variables in Eq 11 are unknown, and our task is to recover the fluid motion $\mathbf{u}$. Considering:

$$-\frac{d\mathbf{q}(0)/dt}{2a(0)} = \mathbf{u} + \eta\mathbf{n}, \quad (12)$$

where η is an unknown scalar defined as $\eta = -\frac{j(1-j)\mathbf{n}^\mathsf{T}\mathbf{u}}{dh}$.

Note that LHS of Eq. 12 is known. Therefore, *we can recover the motion perpendicular to the background*

---

[8]I is the 2×2 identity matrix.

gradient $\mathbf{n}$, *but cannot recover the motion parallel to the background gradient* $\mathbf{n}$, because the scalar η in front of $\mathbf{n}$ is unknown. Note . Moreover, let $\mathbf{n}_\perp$ be the unit vector that is parallel to the background structure (so it is perpendicular to $\mathbf{n}$). Then by multiplying[9] $\mathbf{n}_\perp$ on both sides of Eq. 12, we get the **simplified refractive flow equation**:

$$-\mathbf{n}_\perp^\mathsf{T}\frac{d\mathbf{q}/dt}{2a} = \mathbf{n}_\perp^\mathsf{T}\mathbf{u}. \quad (13)$$

It is easy to show that $-\frac{d\mathbf{q}/dt}{2a}$ is the speed of the center of the observed circular boundary. Thus the simplified refractive flow equation Eq. 13 shows that the motion of the observed image boundary and the motion of the refractive object have the same projection on the direction of background structure $\mathbf{n}_\perp$. Thus we can get the component of refractive motion that is parallel to the background structure by tracking the observed boundary.

This equation also shows that is we cannot recover the component of the motion perpendicular to background structure[10]. This is different from the traditional aperture problem, where it is the component of the motion parallel to the background structure that cannot be estimated.

In a general setup, the Jacobian and Hessian of the refractive field are not scalar matrices, and we have the following refractive flow equation (see the supplementary material for the proof).

Proposition 1 (Refractive flow equation (general)) *At each time point t, we fit a conic curve* $\mathbf{x}^\mathsf{T}A\mathbf{x} + \mathbf{q}^\mathsf{T}\mathbf{x} + 1 = 0$ *to the observed boundary within the aperture, where* $A \in \mathbb{R}^{2\times2}$ *and* $\mathbf{q} \in \mathbb{R}^2$ *are the coefficients of this curve. Then the motion* $\mathbf{u}$ *satisfies the equation,*

$$-\mathbf{q}_\perp^\mathsf{T}\frac{d\mathbf{q}/dt}{2} = (A\mathbf{q}_\perp)^\mathsf{T}\mathbf{u}, \quad (14)$$

where $\mathbf{q}_\perp$ *is a vector perpendicular to* $\mathbf{q}$. *Moreover, we cannot recover the motion along with the vector* $RA\mathbf{q}_\perp$ *just from the observation, where* R *is the* $90°$ *rotation matrix.*

---

[9]We consider $\mathbf{n}_\perp$ as a known variable, as it we can recover the direction of $\mathbf{n}_\perp$ from the observation, since $\mathbf{q}(0) = d^{-1}(1-j)\mathbf{n}$ and $\mathbf{n}_\perp \perp \mathbf{n}$.

[10]Although we only show Eq. 13 is a necessary condition that $\mathbf{u}$ is a solution of the refractive flow problem, it is also a sufficient condition. See the supplementary material for the proof of the sufficiency.
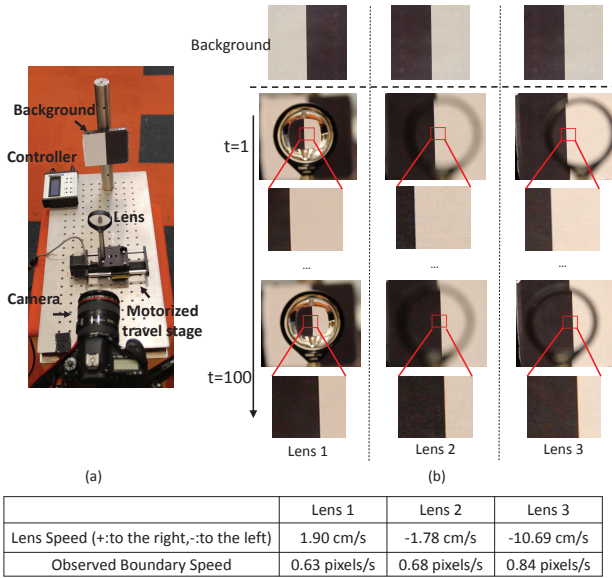
Figure 7. Experiments on three magnifying lenses. (a) Setup. (b) Captured sequence with different lens and background.

	Lens 1	Lens 2	Lens 3
Lens Speed (+:to the right,-:to the left)	1.90 cm/s	-1.78 cm/s	-10.69 cm/s
Observed Boundary Speed	0.63 pixels/s	0.68 pixels/s	0.84 pixels/s

		Lens 1	Lens 2
	Lens speed	1.43 cm/s	2.00 cm/s

(a) Motion of the lens is perpendicular to the background structure

		Lens 1	Lens 2
	Lens speed	2.00 cm/s	2.00 cm/s

(b) Motion of the lens is parallel to the background structure

Figure 8. Experiments on two lenses with significant radial distortion. (a) In both of two sequences, background only contains vertical structure, and both lens are moving to the right. (b) In both of two sequences, background only contains horizontal structure, and both lens are moving to the left.

The ambiguous direction $RA\mathbf{q}_\perp$ in the general refractive flow equation is along the vector connecting the center of the aperture $\mathbf{o}$ to the center of the observed conic curve $\mathbf{o}'$. This is illustrated in Figure 6(c) where the blue arrow indicating the vector $\overrightarrow{\mathbf{o}'\mathbf{o}}$ aligns with the red arrow showing the direction of observed distortion due to the refraction.
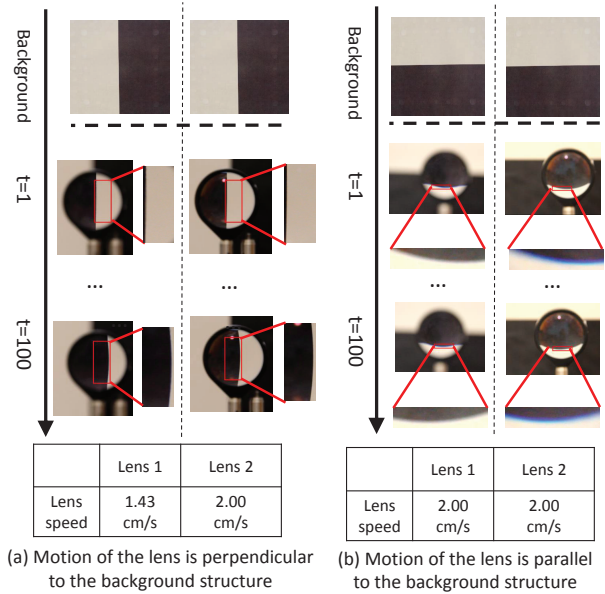
When the refraction effect is mild, this ambiguous direction also approximately equals to the direction of background structure rotated by the Hessian H of refractive field. Note that this ambiguous direction is not always aligned with the background gradient[11]. In Figure 6(c), they are happened to be aligned because H is a scalar matrix.

4. Experiments

In this section, we present experiments that verify the ambiguity theory. Please refer to our website (http://people.csail.mit.edu/tfxue/RefractiveAperture/) for the full sequences and results.

First order observation First, the experiment shown in Figure 7 confirms the claim that by observing a first order structure, it is impossible to infer the motion of a refractive object. In this experiment, a camera views a black and white background through a moving magnifying lens (Figure 7(a)). The lens is mounted on a motorized travel stage, so we can control the speed of the lens. We take three sequences with different backgrounds, lens shapes, and lens speeds, each one corresponding to a column of Figure 7(b). In all these three sequences, a background

---

[11]We define $H = H_x n_x + H_y n_y$.

with vertical boundary is used, but in the first one, the black region is on the right and in the second and the third one, the black region is on the left. The first lens moves to the right, and second and third lenses move to the left. Also, the third one moves faster than the first two. However, the sequences observed through each small aperture (marked by red rectangle) are quite similar, meaning it is impossible to recover the horizontal motion of lens from the observation through the aperture, which is consistent with our theory.

Second order observation In the previous experiment, the aperture is chosen to be very close to the center of the lens, so its refractive field is approximately linear in this region. Thus radial distortion is hardly observed (the observed boundary is a straight line).

To illustrate the ambiguity when the refractive field has non-negligible second-order component, we now use two thick lenses and pick the aperture away from the lens center, so that a significant radial distortion is observed, as shown in Figure 8. Lens 1 has a longer focal length, so that its refractive field has a weaker second order component than that of lens 2.

First, we move these lenses perpendicularly to the background structure (Figure 8(a)). Although they move at different speeds, the observed sequences are quiet similar. This indicates that it is hard to recover the horizontal component of the motion. Next, we move them parallel
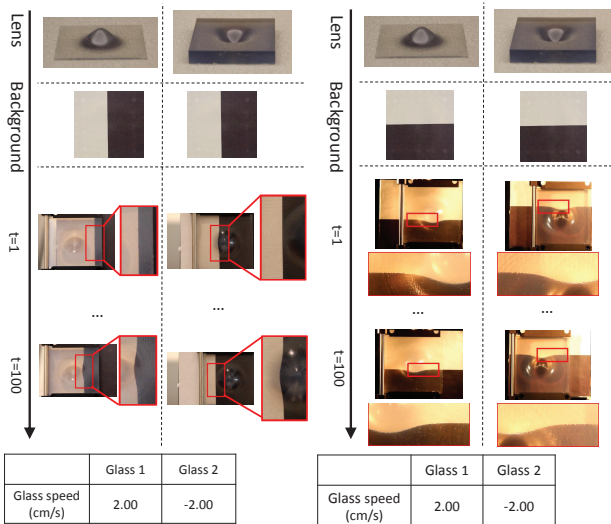
Figure 9. Experiments on 3D-printed Gaussian-shaped glasses.

Figure 10. Experiments on hot air generated by a candle.

to the background structure (Figure 8(b)). Now the observed boundary moves together with the lenses, and to generate two similar sequences, these two lenses must move in the same speed. This experiment shows that we can recover the component of the motion parallel to the background structure, but not the component of the motion perpendicular to it, which is again consistent with our theory.

3D-printed glasses. We also illustrate the ambiguity using Gaussian-shaped glasses, similar to the synthetic experiment shown in Figure 6. We 3D-printed two 3D Gaussian-shaped glasses shown in the first row of Figure 9 and captured four sequences using the same setup as described in Figure 6. We also get the same result as described in Figure 6, that is, the component of the motion perpendicular to the background is hard to estimate (Figure 9(a)), but the component of the motion parallel to the background can be recovered (Figure 9(b)).

Hot air from a candle. At last, we verify our theory by two sequences captured through hot air generated by a burning candle, as shown in Figure 10. The background texture consists of patterns from two color channels. The blue channel of the background is fully-textured, from which we can correctly recover the upward air motion (Figure 10(b,d)), and we consider the recovered motion from this channel as the ground truth. Here we use the algorithm in [31] to calculate the motion of air flow from input sequences. The red channel of background contains texture only in one direction (Figure 10(a,c)). When the texture in red channel is perpendicular to the
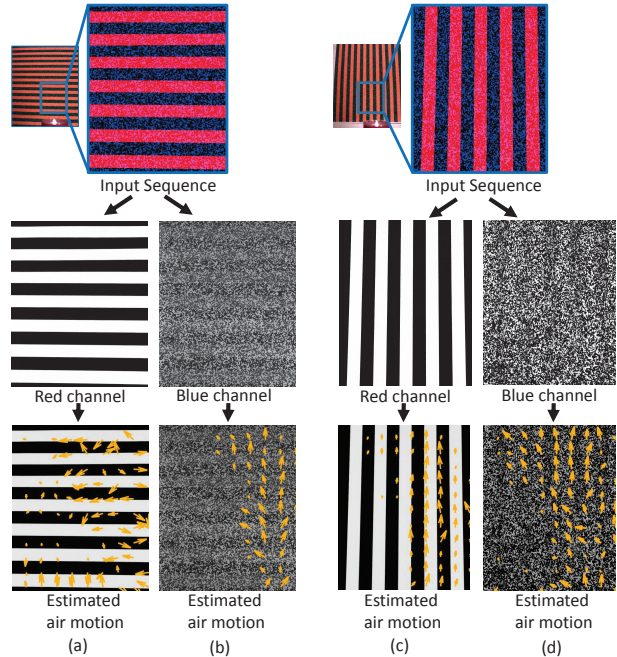
direction of air motion (Figure 10(a)), the estimated motion is incorrect (different from the ground truth motion in Figure 10(b)), and when the background texture is parallel to the direction of air motion (Figure 10(c)), the estimated motion is roughly correct (similar to the ground truth motion Figure 10(d)).

5. Conclusion

In this paper, we analyzed the ambiguity in refractive motion estimation. Many techniques have been proposed to estimate refractive motion from a natural sequence, but none of them discusses the intrinsic ambiguity of the refractive motion estimation from local image information. We analyzed the motion of an unknown refractive object against a stationary background. We studied the constraints that the first and second observation impose on refractive motion. We found that the first order structure in the observed image reveals no information about refractive motion, and the second order structure only reveals the motion in one direction. The derived refractive flow equation also reveals which direction of refractive motion cannot be estimated. Experiments on both solid and fluid refractive objects are shown to verify our theory.

References

[1] Y. Adato, Y. Vasilyev, T. Zickler, and O. Ben-Shahar. Shape from specular flow. *IEEE T-PAMI*, 32(11):2054–2070, 2010. 3

[2] Y. Adato, T. Zickler, and O. Ben-Shahar. Toward robust estimation of specular flow. In *BMVC*, pages 1–11, 2010. 3

[3] E. H. Adelson and J. R. Bergen. Spatiotemporal energy models for the perception of motion. *JOSA A*, 2(2):284–299, 1985. 1

[4] E. H. Adelson and J. A. Movshon. Phenomenal coherence of moving visual patterns. *Nature*, 300(5892):523–525, 1982. 1

[5] R. J. Adrian and J. Westerweel. *Particle image velocimetry*. Cambridge University Press, 2011. 2

[6] S. Agarwal, S. P. Mallick, D. Kriegman, and S. Belongie. On refractive optical flow. In *ECCV*, pages 483–494. Springer, 2004. 2, 3

[7] M. Alterman, Y. Y. Schechner, P. Perona, and J. Shamir. Detecting motion through dynamic refraction. *IEEE T-PAMI*, 35(1):245–251, 2013. 2

[8] M. Alterman, Y. Y. Schechner, and Y. Swirski. Triangulation in random refractive distortions. In *ICCP*, pages 1–10. IEEE, 2013. 3

[9] M. Alterman, Y. Y. Schechner, M. Vo, and S. N. G. Passive tomography of turbulence strength. In *ECCV*. IEEE, 2014. 2

[10] J. L. Barron, D. J. Fleet, and S. S. Beauchemin. Performance of optical flow techniques. *International Journal of Computer Vision*, 12(1):43–77, 1994. 1

[11] M. Ben-Ezra and S. K. Nayar. What does motion reveal about transparency? In *ICCV*, pages 1025–1032. IEEE, 2003. 3

[12] G. D. Canas, Y. Vasilyev, Y. Adato, T. Zickler, S. Gortler, and O. Ben-Shahar. A linear formulation of shape from specular flow. In *ICCV*, pages 191–198. IEEE, 2009. 3

[13] Y. Ding, F. Li, Y. Ji, and J. Yu. Dynamic fluid surface acquisition using a camera array. In *ICCV*, pages 2478–2485, 2011. 3

[14] G. Elsinga, B. Van Oudheusden, F. Scarano, and D. Watt. Assessment and application of quantitative schlieren methods: Calibrated color schlieren and background oriented schlieren. *Experiments in Fluids*, 36(2):309–325, 2004. 2

[15] E. Goldhahn and J. Seume. The background oriented schlieren technique: sensitivity, accuracy, resolution and application to a three-dimensional density field. *Experiments in Fluids*, 43(2-3):241–249, 2007. 2

[16] M. J. Hargather, M. J. Lawson, G. S. Settles, and L. M. Weinstein. Seedless velocimetry measurements by schlieren image velocimetry. *AIAA journal*, 49(3):611–620, 2011. 2

[17] M. J. Hargather and G. S. Settles. Natural-background-oriented schlieren imaging. *Experiments in fluids*, 48(1):59–68, 2010. 2

[18] D. R. Jonassen, G. S. Settles, and M. D. Tronosky. Schlieren "piv" for turbulent flows. *Optics and Lasers in Engineering*, 44(3):190–207, 2006. 2

[19] G. Meier. Computerized background-oriented schlieren. *Experiments in Fluids*, 33(1):181–187, 2002. 2

[20] N. J. Morris and K. N. Kutulakos. Dynamic refraction stereo. In *ICCV*, volume 2, pages 1573–1580. IEEE, 2005. 3

[21] M. Raffel, C. Tung, H. Richard, Y. Yu, and G. Meier. Background oriented stereoscopic schlieren (BOSS) for full scale helicopter vortex characterization. In *International Symposium on Flow Visualization*, 2000. 2

[22] H. Richard and M. Raffel. Principle and applications of the background oriented schlieren (bos) method. *Measurement Science and Technology*, 12(9):1576, 2001. 2

[23] M. C. Roggemann, B. M. Welsh, and B. R. Hunt. Imaging through turbulence. 1996. 3

[24] P. Ruhnau, T. Kohlberger, C. Schnrr, and H. Nobach. Variational optical flow estimation for particle image velocimetry. *Experiments in Fluids*, 38(1):21–32, 2005. 2

[25] G. S. Settles. *Schlieren and Shadowgraph Techniques: Visualizing Phenomena in Transparent Media*. Springer, 2001. 2

[26] G. S. Settles. The penn state full-scale schlieren system. In *International Symposium on Flow Visualization*. Notre Dame University, IN, 2004. 2

[27] B. R. Sutherland, S. B. Dalziel, G. O. Hughes, and P. Linden. Visualization and measurement of internal waves by synthetic schlieren. part 1. vertically oscillating cylinder. *Journal of Fluid Mechanics*, 390(1):93–126, 1999. 2

[28] Y. Swirski and Y. Y. Schechner. 3Deflicker from motion. In *ICCP*, pages 1–9. IEEE, 2013. 3

[29] Y. Tian and S. G. Narasimhan. Seeing through water: Image restoration using model-based tracking. In *ICCV*, pages 2303–2310. IEEE, 2009. 3

[30] L. Venkatakrishnan and G. Meier. Density measurements using the background oriented schlieren technique. *Experiments in Fluids*, 37(2):237–247, 2004. 2

[31] T. Xue, M. Rubinstein, N. Wadhwa, A. Levin, F. Durand, and W. T. Freeman. Refraction wiggles for measuring fluid depth and velocity from video. *ECCV*, 2014. 2, 3, 8

[32] J. Ye, Y. Ji, F. Li, and J. Yu. Angular domain reconstruction of dynamic 3D fluid surfaces. In *CVPR*, pages 310–317, 2012. 3

[33] X. Zhu and P. Milanfar. Removing atmospheric turbulence via space-invariant deconvolution. *T-PAMI*, 35(1):157–170, 2013. 3